



## Smartphone-based colorimetric sensor application for measuring biochemical material concentration

Taif Alawsi<sup>a,b,\*</sup>, Gabriele Proietti Mattia<sup>a</sup>, Zainab Al-Bawi<sup>b</sup>, Roberto Berald<sup>a</sup>

<sup>a</sup> La Sapienza University of Rome, Rome, Italy

<sup>b</sup> Institute of Laser for Postgraduate Studies, University of Baghdad, Baghdad, Iraq



### ARTICLE INFO

**Keywords:**  
Smartphone sensors  
Colorimetric analysis  
Android application

### ABSTRACT

In this paper, colorimetric analysis for biochemical samples has been realized, by developing an easy-to-use smartphone colorimetric sensing android application that can measure the molar concentration of the biochemical liquid analyte. The designed application can be used for on-site testing and measurement. We examined three different biochemical materials with the application after preparation with five different concentrations and testing in laboratory settings, namely glucose, triglycerides, and urea. Our results showed that for glucose triglycerides, and urea the absorbance and transmittance regression coefficient ( $R^2$ ) for the colorimetric sensing application were 0.9825, and 0.9899; 0.9405 and 0.9502; 0.9431 and 0.8597, respectively. While for the spectrophotometer measurement the ( $R^2$ ) values were 0.9973 @560 nm and 0.9793 @600 nm; 0.952 @620 nm and 0.9364 @410 nm; 0.9948 @570 nm and 0.9827 @530 nm, respectively. The novelty of our study lies in the accurate prediction of multiple biochemical materials concentrations in various lightning effects, reducing the measurement time in an easy-to-use portable environment without the need for internet access, also tackling various issues that arise in the traditional measurements like power consumption, heating, and calibration. The ability to convey multiple tasks, prediction of concentration, measurement of both absorbance and transmittance, with error estimation charts and ( $R^2$ ) values reporting within the colorimetric sensing application as far as our knowledge there has not been any application that can provide all the capabilities of our application.

### 1. Introduction

Recent advancements in smartphone technologies enable multiple scientific disciplines to apply this technology in serving their needs. Lab-on-Chip (LoC) is increasingly used to rely on smartphone sensors to make on-site laboratory testing, measurement, and diagnostics [1]. Smartphone complementary metal-oxide-semiconductor (CMOS) camera is a big resource for information gathering and with the help of smart applications for image processing and data analysis, the concept of rapid testing has been realized [2]. Traditional laboratory techniques for testing and diagnosis of analytes by bulk instruments and devices with careful specialists are still in place, however, designing smartphone-based instruments and applications is rising significantly in recent years this is due to many factors such as easy-to-use applications, portability of the whole system, cost-effectiveness, easy-manufacturing, rapid testing and diagnosis, an extremely comparable performance which allows the functionality in rural areas and thus makes the smartphone-based approach more convenient in many cases [3].

Usually, there are two approaches to tackle the problem of diagnosis and testing, one is based on designing both hardware and software components to establish a strong link between them and get a reliable result. While the other approach involves just developing the software for the smartphone to analyze the different aspects of the image and perform the required processing as we present here in this article [4,5]. Biochemical materials, nanomaterials, and hazardous materials were investigated, analyzed, and tested with the smartphone-based approach to naming a few, glucose [6–8], c-reactive protein [9], gold nanoparticles [10], nitrite [11,12], chromium [13,14], iron [14], mercury [15]. The concentration measurement is a key element in characterizing the material behavior, for example, in environmental protection, usually, the materials should be at a certain level of concentration when this exceeds the appropriate amount it leads to hazardous situations such as poisoning, fatigue, and death of certain species. Many materials show a colorimetric behavior when prepared for a certain concentration and this concentration is marked somehow into the intrinsic color produced by the material under a certain concentration, sometimes naked eyes can

\* Corresponding author at: La Sapienza University of Rome, Rome, Italy.

E-mail addresses: [taif.alawsi@uniroma1.it](mailto:taif.alawsi@uniroma1.it), [taif.alawsi@ilps.uobaghdad.edu.iq](mailto:taif.alawsi@ilps.uobaghdad.edu.iq) (T. Alawsi).

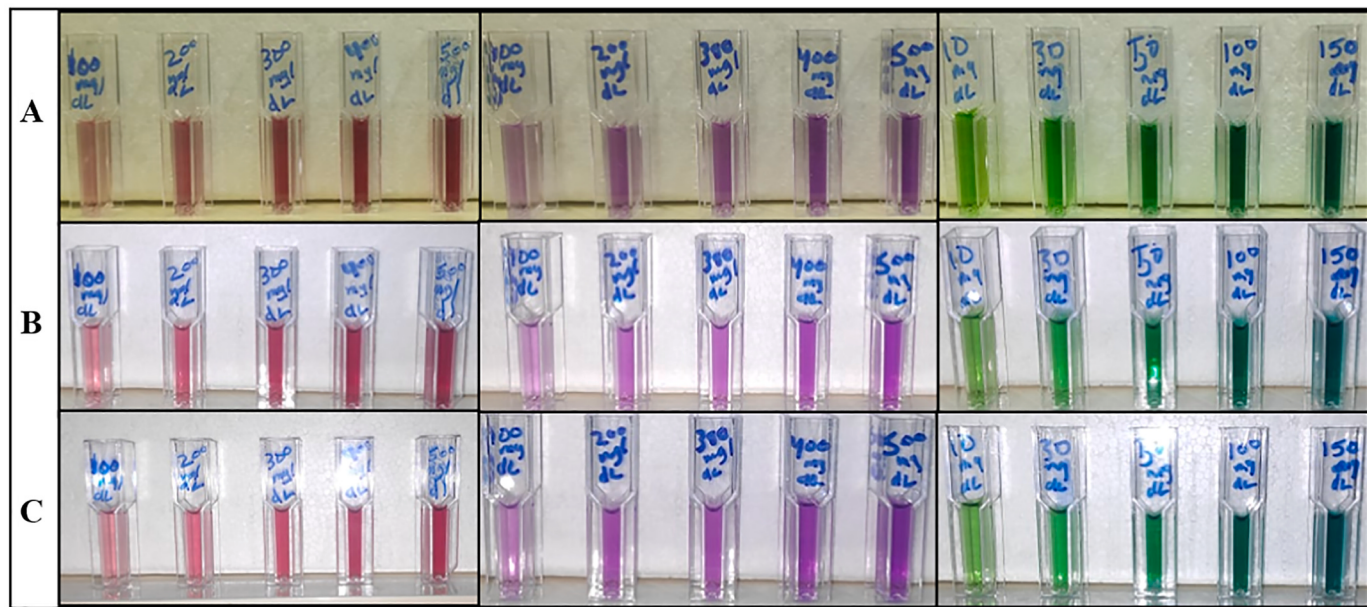


**Fig. 1.** Images of biochemical samples captured by Xiaomi Pocophone F1 (12 Mpx); glucose (Pink; left side images) triglycerides (Purple; middle images) urea (Green; right-side images) at 20 cm distance (a) without flash and no reflection (b) with flash (b) with flash and reflection.

distinguish between certain levels of concentration due to color change, but in most cases, it is hard to predict the concentration with naked eyes. The solution is to analyze the color of the material by introducing image processing and smart applications this is the concept of colorimetric analysis [16–18]. Alternative approaches can be based on fluorescence [19], chemiluminescence [20,21], luminescence [22], phosphorescence [23] and bioluminescence [24]. In 2014, Ruiz, et al., [12], used image processing and android mobile application to calculate nitrite ( $\text{mg} \cdot \text{L}^{-1}$ ) concentration based on HSV (Hue, Saturation, and Value) color model for paper microfluidic devices. Also, Hong and Chang [25] developed a mobile application for colorimetric sensing of multi-analyte arrays. The smartphone identifies the position of the sensor then the colors measured at each sensor are digitized based on a correction algorithm; leading to concentration values by pre-loaded calibration curves. Additionally, Firdaus, et al. [14] used two methods for digital image colorimetry to determine the concentration of iron and chromium materials, the methods were for postprocessing the images in MATLAB namely, simple linear regression for an individual (Red, Green, and Blue) RGB channel and partial least square for all channels of RGB image. In 2015, Jung, et al., [26], detected saliva alcohol concentration using Smartphone-based colorimetric RGB and HSV analysis. They used separate channels of color intensity values for Ethyl alcohol concentration in percentages. In 2017, Mutlu, et al., [27] used a machine learning algorithm in smartphone-based colorimetric detection of pH values with different types of images JPEG, RAW, and RAW-corrected. Their approach is applicable for paper-based colorimetric assays. In 2018, Guo, et al., [28], designed a 3D smartphone adapter for colorimetric sensing of formaldehyde, using the images for different formaldehyde concentration samples, their results focus on the color ratio of the reaction region. The formaldehyde concentrations were in ppm (part per million) that were plotted against the color ratio for different concentrations. They used individual color channels to show their results, the red, green, and blue channels. Also, Soni, et al. [29] developed a smartphone-based handheld optical biosensor for the determination of urea in saliva. The sensitivity reported was  $-0.005 \text{ average pixels sec}^{-1}/\text{mgdL}^{-1}$  with a (limit of detection) LOD of  $10.4 \text{ mgdL}^{-1}$ . In 2019, Zhong, et al., [10] developed a smartphone-based colorimetric sensor with a combination of gold nanoparticles and enzyme-linked immunosorbent assay (ELISA) technique on a 3D portable adaptor to detect saxitoxin poison in seafood. They present their result as individual channels of

RGB images from the ELISA kit. In 2020, Xing, et al. [21] developed a dual-functional smartphone-based sensor for colorimetric and chemiluminescence detection. In colorimetry, five analytes that display different colors and various intensities were detected sensitively while in chemiluminescence  $\text{H}_2\text{O}_2$  was detected successfully. They created a smart application that allows testing and sharing of fluoride quantification results with a 3D printed smartphone adapter for RGB image detection and processing.

## 2. Materials and methods

We used the following biochemical materials, glucose (BioSystems Co., 11,503, Barcelona, Spain), triglycerides (Agappe Diagnostics, 11,410,103, Cham, Switzerland), and urea (BioSystems Co., 11,536, Barcelona, Spain) control samples with five different concentrations, resulting in fifteen total samples, as shown in Fig. 1 and Fig. S.1 (in the supplementary material). To prepare glucose samples, add 1 mL of glucose reagent A (BioSystems Co., 11,503, Barcelona, Spain), then add 10  $\mu\text{L}$  of glucose standard solution of 100 mg/dL, then incubate for 10 min. in a water bath. For triglycerides samples, adding 1 mL of triglyceride reagent S.L. (Agappe Diagnostics, 11,410,103, Cham, Switzerland), then adding 5  $\mu\text{L}$  of triglyceride standard solution of 200 mg/dL, then 10 min. Incubation in a water bath. Urea samples were prepared by adding 0.5 mL of urea reagent A1 (BioSystems Co., 11,536, Barcelona, Spain), then the addition of 20  $\mu\text{L}$  urea standard solution of 50 mg/dL, after that incubating in a water bath for 10 min., then adding 2 mL of urea reagent B, finally 10 min. Incubation in a water bath. The prepared samples employ the use of Eq. (1) below:

$$C_1 V_1 = C_2 V_2 \quad (1)$$

Where:  $C_1$ : Original concentration;  $V_1$ : Original volume;  $C_2$ : Prepared concentration;  $V_2$ : Prepared volume. We measured the sample transmittance ( $T$ ) and absorbance ( $A$ ) with a spectrophotometer (Chongqing Gold Mechanical & Electrical Equipment Co., Ltd., GD-725, Chongqing, China), and for each measured value of sample absorbance and transmittance we compute the other value to check for the error of measurement using Eqs. (2.a) and (2.b) below:

$$A = 2 - \log_{10}(T\%) \quad (2.a)$$

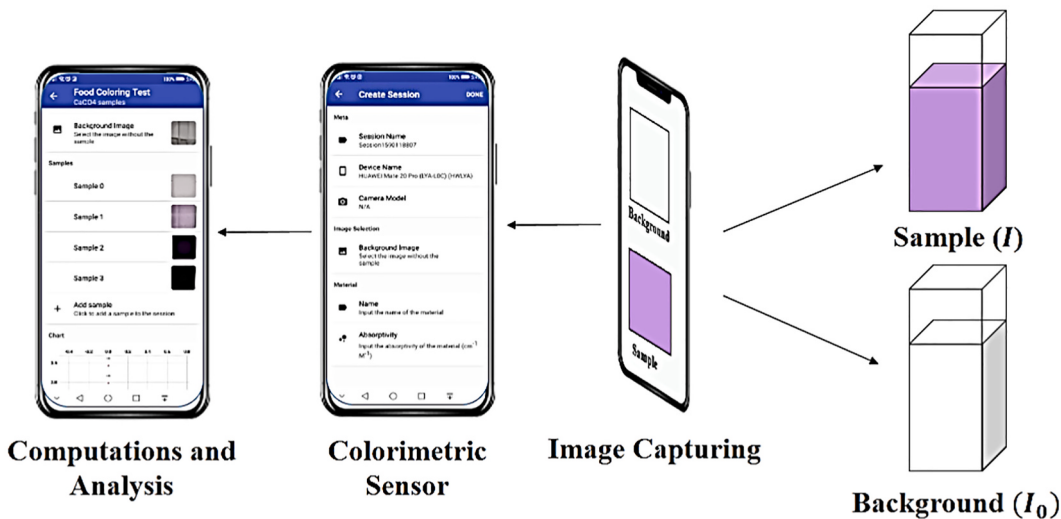


Fig. 2. Schematic illustration of the imaging mechanism showing both background and sample image

$$T\% = 10^{2-A}$$

And since the absorbance is equal to [2]:

$$A = \varepsilon(\lambda)bc \quad (3)$$

Where:  $\varepsilon(\lambda)$ : Molar absorptivity; b: Sample length; c: Sample concentration, and Since [2]:

$$A = -\log_{10} (I_0/I) \quad (4)$$

Combining Eq. (3) with (4), we get:

$$I = I_0 \exp.^{-\varepsilon(\lambda)bc} \quad (5)$$

Where:  $I_0$ : Background intensity of the RGB colored image; I: Sample intensity of the RGB colored image. The absolute average error percentage (err%) between measured quantities of transmittance and absorbance for the sample is calculated as shown in Eqs. (6.a) and (6.b)

$$(2.b)$$

$$err\% = \sum_{n=1}^N \frac{|T_M - T_C|_n}{N} \% \quad (6.a)$$

$$err\% = \sum_{n=1}^N \frac{|A_M - A_C|_n}{N} \times 100\% \quad (6.b)$$

Where: n: Integer; N: Number of samples; the subscripts M and C denote the measured and calculated quantities respectively. We can compute sample concentration in the developed Android application (Colorimetric Sensing) in two different units, mg/dL and (mM) using these formulas for glucose Eqs. (7.a) and (7.b), for triglycerides Eqs. (7.c) and (7.d), and for urea Eqs. (7.e) and (7.f).

$$1 \text{ mM} = 18.0182 \text{ mg/dL} \quad (7.a)$$

$$1 \text{ mg/dL} = 0.055 \text{ mM} \quad (7.b)$$

$$1 \text{ mM} = 88.57 \text{ mg/dL} \quad (7.c)$$

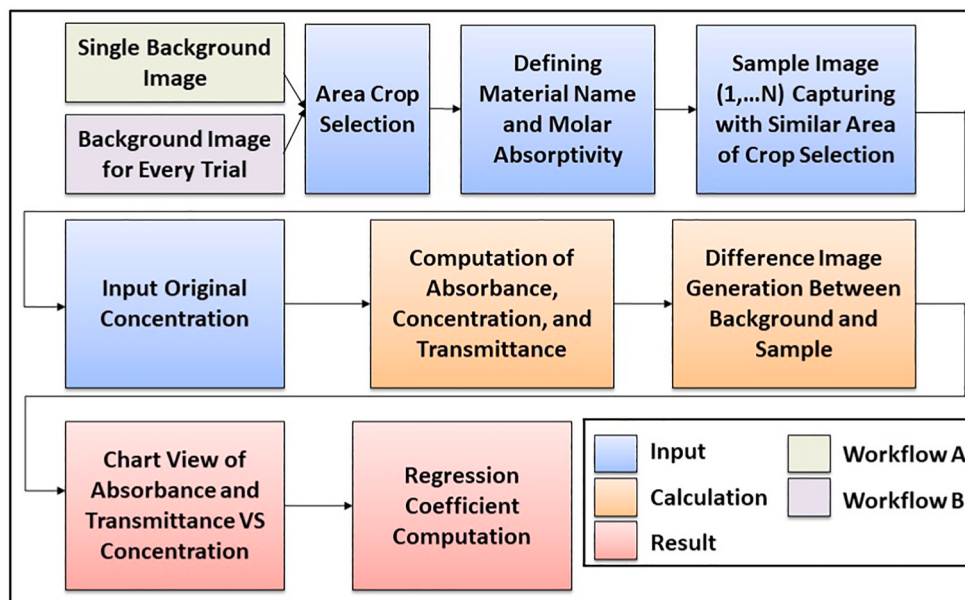
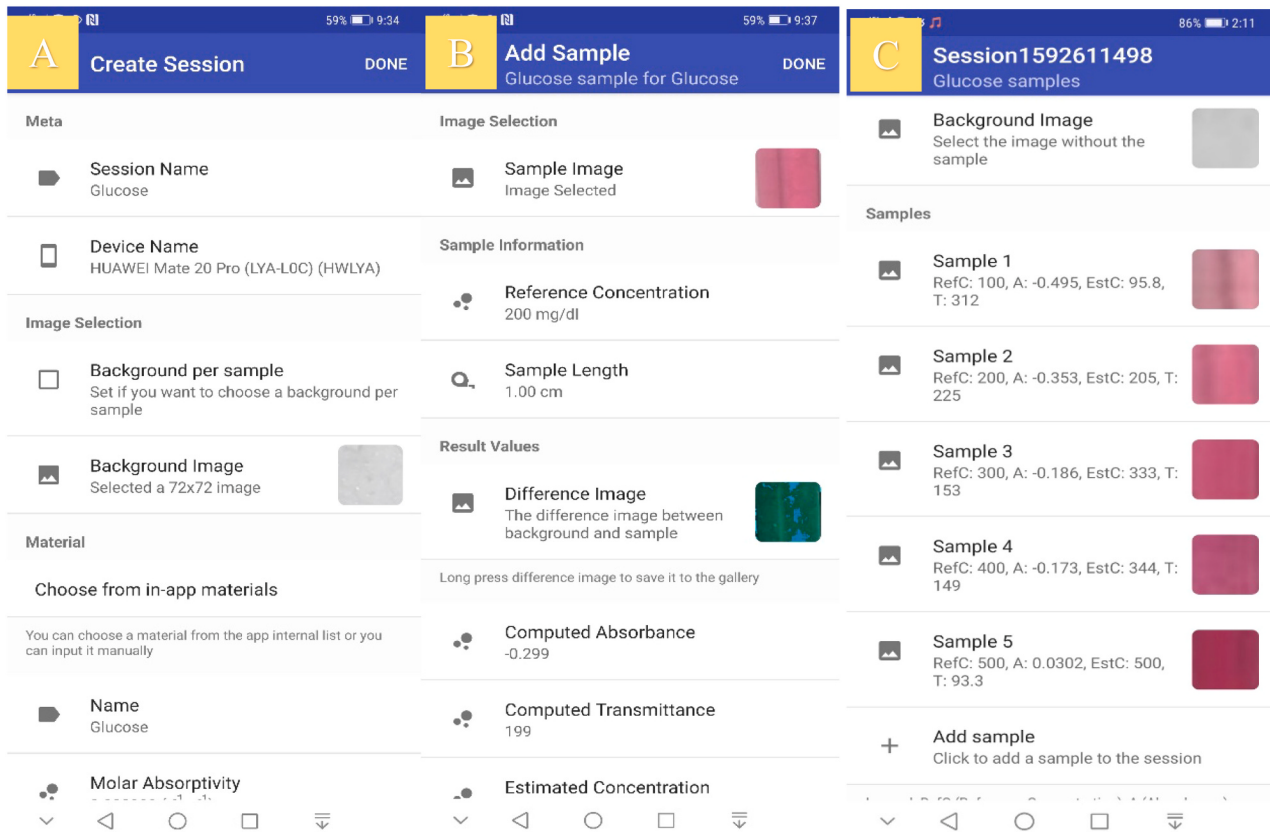


Fig. 3. Colorimetric sensing application workflows (A) with a single image background (light green box) (B) with a background image for every trial (light purple box).



**Fig. 4.** Colorimetric sensing application layout (a) Creating a session (b) Adding a sample (c) List of samples with the same material in different concentrations.

$$1 \text{ mg/dL} = 0.01129 \text{ mM}$$

(7.d)

$$1 \text{ mM} = 6.01 \text{ mg/dL}$$

(7.e)

$$1 \text{ mg/dL} = 0.17 \text{ mM}$$

(7.f)

The Colorimetric Sensing computes the intensity values based on the RGB images for both background and sample following Eq. (8).

$$I_R = \log_{10} R_0/R_S$$

$$I_G = \log_{10} G_0/G_S$$

$$I_B = \log_{10} B_0/B_S$$

$$I_{\text{total}} = (I_R + I_G + I_B)/3$$

Where: the subscripts  $0$ , and  $S$  represent the background and sample,  $R$ : Red channel;  $G$ : Green channel;  $B$ : Blue channel of the RGB image. Then we can estimate the error of computation which gives us the regression coefficient ( $R^2$ ), which serves as the measurement accuracy factor, the experimental setup is illustrated in (Fig. 2).

### 3. Experimental work

Here we will discuss the developed application, the application can proceed in two different workflows A and B. (Fig. 3) shows the application workflow A and B. We designed and implemented an Android application, that we will call “Colorimetric Sensing”, using the latest version of Android Studio (4.0). The role of the application is to implement the equations provided in the Material and Methods section (Eqs. (2)–(8)) but offering a user-friendly interface. Colorimetric Sensing was written in Kotlin and was tested successfully on a Huawei Mate 20

Pro (Huawei manufacturing, China). Fig. 4 shows the two workflows that the user can follow for generating results: the first one, workflow A, allows to use of the same background image for all the samples, the second one, workflow B allows the user to choose it for every trial of sample measurement. We now describe workflow A, then workflow B will easily follow from that. (1) The user creates a new session (Fig. 4a), the session can be considered as a container of all samples of the same type, for this reason when creating it the user must choose the material of interest, its absorptivity, and the linear fit when needed. The user can choose from a fixed list of materials that we implemented from the “Handbook of Laser Dyes” [30] but he can also manually provide the material metadata. In this workflow, the user is now asked to choose the background image that will be used for all the samples in the session. (2) Once the user has created a session, he can start to add samples, so he opens the session dashboard (Fig. 4b) and adds a new sample (Fig. 4c). The sample image can be either already in the smartphone storage or it can be taken instantaneously from the smartphone camera. After choosing the image, the user chooses (3) the area of the image that will be used for the analysis, this area will be forced to be of the same size as the previously selected background, in order to avoid bad concentration predictions due to different image resolution. After the image selection, the user can immediately see the concentration predictions (in two units: molar concentration (Mol.) and milligram per deciliter ( $\text{mg.dL}^{-1}$ )) using the conversion formula (7.a and 7.b), the RGB difference between the background image and the sample image and also input a value for the sample length (if it is not matching the standard 1 cm). Finally, after processing many samples of the material, the user (4) can see the absorbance, transmittance, and error estimation curves inside the application with the value of the regression coefficient ( $R^2$ ) is indicated for both curves of absorbance and transmittance with linear approximation curve and the points represent the actual data collected by the application (see Fig. 6b). Moreover, the application also draws



**Fig. 5.** Samples of calculations using the colorimetric sensing application (A) glucose sample list (B) triglycerides sample list (C) urea sample list (D) calculations of absorbance (E) transmittance (F) error of measurements.

prediction error charts if the user wants to compare them with a laboratory device.

#### 4. Results

The transmittance, absorbance, and the absolute average error curves for glucose (350–640 nm), triglycerides (400–680 nm), and urea (500–780 nm) with concentrations of (100, 200, 300, 400, 500 mg/dL) for glucose and triglycerides, while the urea concentrations were (10, 30, 50, 100, 150 mg/dL) are shown in the supplementary materials (Figs. S.2, S.3, and S.4). Trials of glucose, triglycerides, and urea were conducted for each material, we captured 3 high-resolution photos that were processed and a fourth trial was made by changing the background of the third photo for all materials to establish both application workflows (A) and (B) (Fig. 3). The number of trials was 15, in each trial, the position of the selected portion of the image differs slightly and thus making a change in the absorbance reading and thus the concentration estimation in the app. The overall number of trials for all materials in all

images was 900 trials. We used both the absorbance and the transmittance for convenience, as shown in (Fig. 5) where background image, samples, concentration estimation, plots of transmittance and absorbance for all samples versus concentration in two different units, the error of measurement bar chart and the linear regression coefficient ( $R^2$ ) for both A and T is depicted by the colorimetric sensing application.

(Figs. 6 and 7) show the absorbance and the transmittance curves for the glucose, and triglycerides materials both calculated in the colorimetric sensing application and measured in the spectrophotometer, respectively.

(Fig. 8) presents the absorbance and the transmittance curves for the urea material both calculated in the colorimetric sensing application and measured in the spectrophotometer.

#### 5. Discussion

Our approach in this study was a mixture of laboratory measurements of the biochemical materials, glucose, triglycerides, and urea (see

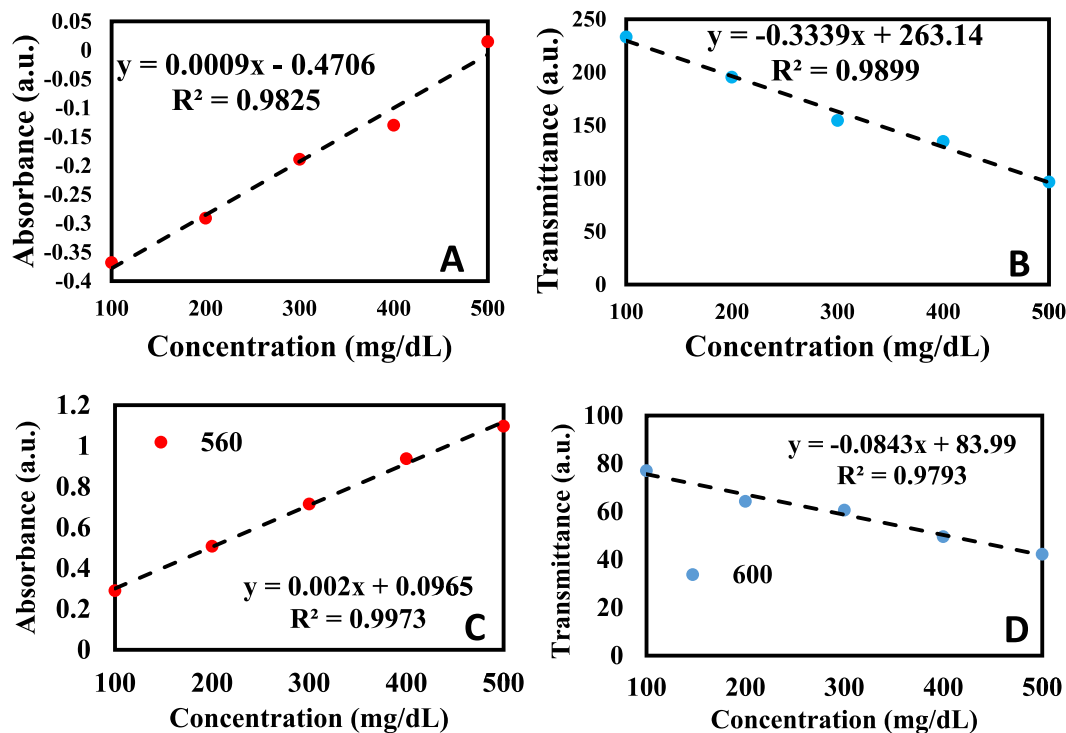


Fig. 6. Application-based results for glucose (a) Absorbance (b) Transmittance. Spectrophotometer-based results (c) Absorbance (d) Transmittance.

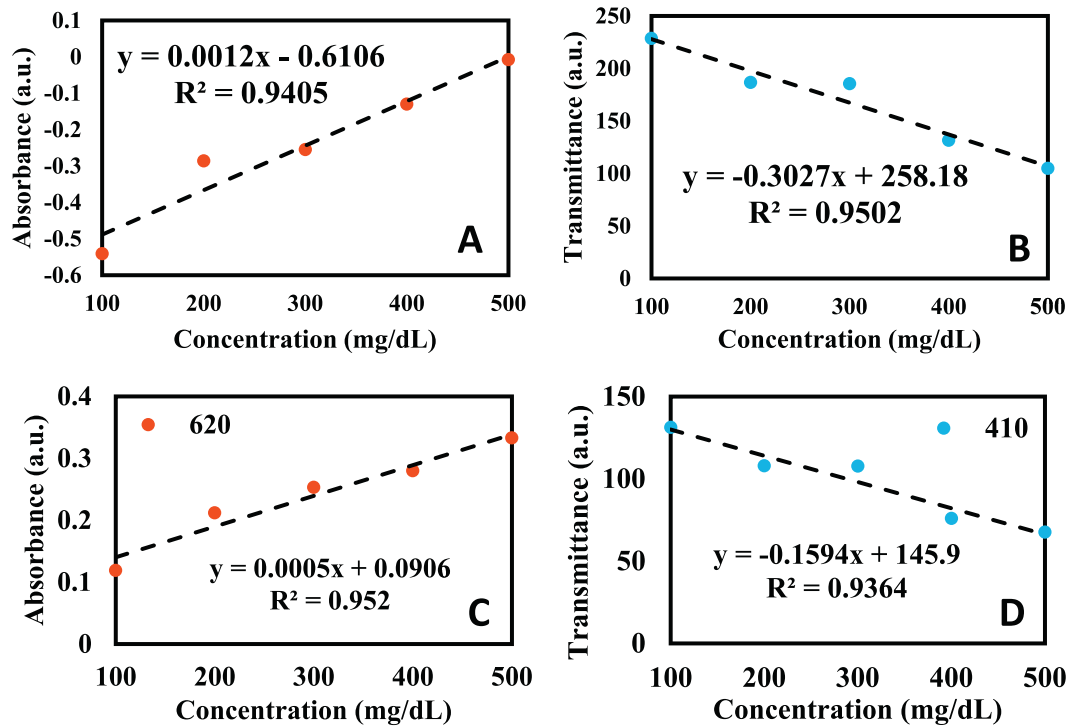
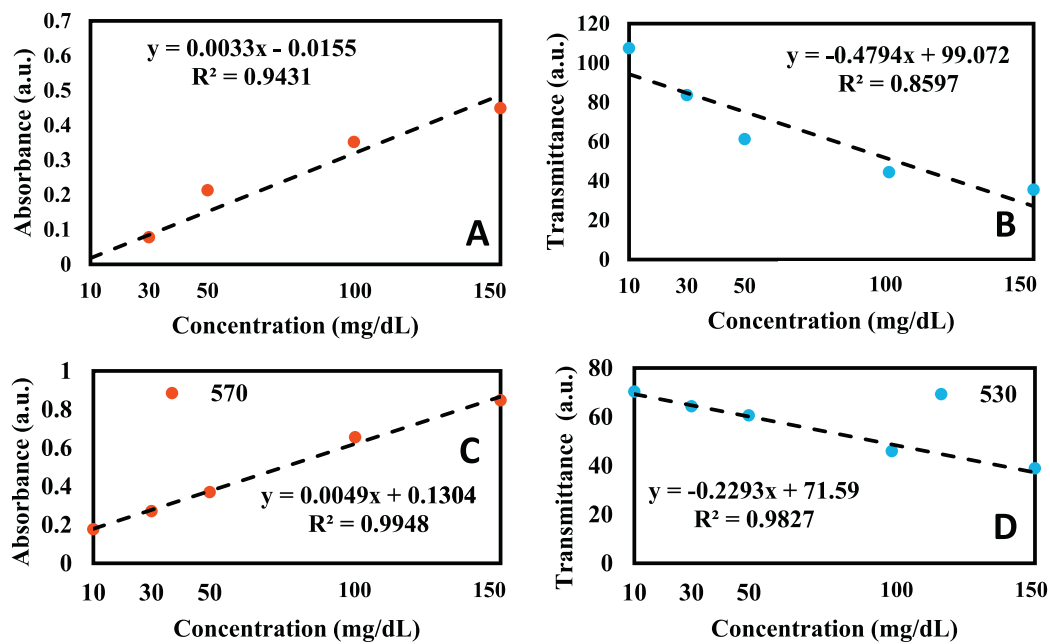


Fig. 7. Application-based results for triglycerides (a) Absorbance (b) Transmittance. Spectrophotometer-based results (c) Absorbance (d) Transmittance.

Fig. 1 and Fig. S.1 (in the supplementary material)). In addition to using the developed colorimetric sensing application for testing and measurement (see Figs. 4 and 5). The prepared concentrations of all the samples reported here were control samples. For triglycerides, the use of a wide range of concentrations is due to the fact that in 100 mg/dL concentration is a normal value of triglycerides concentration in human, a 200 mg/dL concentration is a borderline high level, 300 mg/dL and

400 mg/dL are high levels, finally, 500 mg/dL is very high level. These high levels come from certain conditions including obesity, low thyroid hormones, diabetes with poor control, liver and kidney diseases, alcohol consumption, and poor diet. A rare case of 10,000 mg/dL was found in the literature [31] also this justifies the use of the high concentration levels [32–35]. We took into account many variables that may arise from dealing with the images of the biochemical materials. The images were



**Fig. 8.** Application-based results for urea (a) Absorbance (b) Transmittance. Spectrophotometer-based results (c) Absorbance (d) Transmittance.

taken by Xiaomi Pocophone F1 (12 Mpx) under different lighting circumstances, with flash, reflection, and without flash to estimate the best available environment for concentration measurements. The designed application here can overcome different lighting conditions of the samples by inserting the fitting parameter to the application, in which, the molar absorptivity can be calibrated regardless of the illumination light type. This is shown as in Fig. 1, different lighting parameters were chosen to check for the practicality of the application to predict the concentrations of the materials under different lightening circumstances, so even when different environmental lighting is the case, the application by simple calibration of the data can overcome this issue. Therefore, discussion of different LED sources and CMOS camera characteristics are not the case, since the application work by simple calibration with a priori determined concentration values, and then the application can predict the unknown concentration of the material. To put it in different words, we can say that in order to accurately predict the concentrations of unknown samples, first, a known value must be at hand and then calibrated for the unknown material. And since we are developing the application from scratch with no previous data at hand, we are making the prediction goes more automated by the application by loading data into the application in which the application can predict the unknown concentrations with high accuracy. The colorimetric sensing application can work with more materials other than just the three materials reported here. So, we used the handbook of laser dyes [30] to add all the materials that are discussed by the handbook into the application library for potential use in other samples. This is to justify that the application can be preloaded with actual measured molar absorptivity data and also can be calibrated for other data. And since we could not find detailed and trustworthy information about the materials that we are using in the manuscript, we worked by calibration and known concentration approach. The images taken were high-resolution images with a pixel size of (without flash  $960 \times 540$ ) and (with flash  $528 \times 960$ ) therefore the estimation of the concentration was close to the actual concentration. We verified the laboratory measurement based on Eqs. (2.a) and (2.b)) after preparation with high accuracy of the material concentration in laboratory settings. The laboratory measurements were done in the visible region of the spectrum; for glucose  $\lambda = (350\text{--}640\text{ nm})$ , triglycerides  $\lambda = (400\text{--}680\text{ nm})$ , and urea  $\lambda = (500\text{--}780\text{ nm})$ . We provided the error of measurements based on comparing each recorded value for absorbance and transmittance with the equation-

based value (2.a and 2.b) of the measured quantity. The error was marginal as shown in the supplementary material (see Figs. S.2c, S.3c, and S.4c). The absorbance and transmittance curves show the one-to-one mapping of the measured concentration, with a linear increase in absorbance and linear decrease in transmittance for all inspected materials (Figs. 6, 7, and 8). For the designed application, we examined different circumstances, for example, we took into account the selected area of image processing to be the critical issue since in each trial of computation when choosing the material this area is subjected to minor deviation, and thus careful choice should be made when dealing with the samples. The nature of the processed images in terms of lightening is also important and we considered it when designing with the application, by taking three different scenarios of image lightening (with flash, with flash, and reflection, without flash) (see Fig. 1). Finally, the background image choice is subjected to an accurate selection of the position of the pixels and cropped image size, we provided the opportunity in the colorimetric sensing application to deal with background images in two different ways. The workflow (A) with single image background for all samples provides a solution for image comparison by subjecting all samples to the same background, this eliminates the need for background image set up every trial, reducing the error of measurements, and provides faster image processing resulting in a rapid testing environment by reducing the processing time of concentration measurement. On the other hand, workflow (B) with background image for every trial is useful in other cases, for example, when the user prepares the samples in different timeframes or different lightening and positioning of the cuvette, this results in changes in the background image, thus, the workflow (B) solves the issue with high accuracy. The results were promising since we get for the colorimetric sensing application a linear regression coefficient ( $R^2$ ) values for absorbance and transmittance for glucose, triglycerides, and urea 0.9825, and 0.9899; 0.9405 and 0.9502; 0.9431 and 0.8597, respectively (see Figs. 6.a, b, 7.a, b, 8.a, and b). While for the spectrophotometer measurements the ( $R^2$ ) of the absorbance and transmittance with the same material flow was 0.9973 @560 nm and 0.9793 @600 nm; 0.952 @620 nm and 0.9364 @410 nm; 0.9948 @570 nm and 0.9827 @530 nm, respectively (see Figs. 6.c, d, 7.c, d, 8.c, and d). These results indicate a very good linear behavior and the estimation of the concentration for the materials was valid ( $>0.9$  [5]) for testing purposes. The linearity of the samples in a laboratory setting is different from the linearity of the image processing. A

**Table 1**

Comparison of different methods, and approaches in various techniques of concentration measurements.

Material	Concentration Unit	Measured Quantity	R <sup>2</sup>	Ref
Glucose	mg.dL <sup>-1</sup>	Normalized G signal	0.983	[6]
Bicinchoninic acid; Glucose	mg.mL <sup>-1</sup> ; $\mu\text{mol.L}^{-1}$	Absorbance @certain $\lambda$	0.9939@450; 0.9937@450	[10]
Chromium (VI); Iron (III)	mg.L <sup>-1</sup>	Effective Intensity (R, G, B) channels	0.4174, 0.9962, 0.9946; -0.854; 0.9882; 0.9935	[14]
Phosphate	ppb	Corrected fluorescence	0.96	[19]
Fluoride;	mg.L <sup>-1</sup>	Absorbance	0.9962	[21]
Gaseous formaldehyde	ppm	Color ratio	0.996	[28]
Sulfonamides	$\mu\text{g.mL}^{-1}$	Absorbance	0.996	[37]
Common household dyes; Nitrate	mg.mL <sup>-1</sup> ; ppm	Absorbance @certain $\lambda$	0.998@525; 0.9946@545	[38]
p-nitroaniline; Brilliant Blue	mM; % w/w	Absorbance @certain $\lambda$	0.9975@430; 0.9848@630	[39]
CuSO <sub>4</sub>	M	Absorbance	0.996	[40]
Water content in ethanol	% v/v	Absorbance	—	[41]
Various chemical solvents	mM	Absorbance ratio @certain $\lambda$ and T	@543/@638; @20 °C	[42]
Glucose, Triglycerides, Urea	mg.dL <sup>-1</sup>	Absorbance	0.9825; 0.9405; 0.9431	*
Glucose, Triglycerides, Urea	mg.dL <sup>-1</sup>	Absorbance @certain $\lambda$	0.9973@560; 0.952@620; 0.9948@570	*
Glucose, Triglycerides, Urea	mg.dL <sup>-1</sup>	Transmittance	0.9899; 0.9502; 0.8597	*
Glucose, Triglycerides, Urea	mg.dL <sup>-1</sup>	Transmittance @certain $\lambda$	0.9793@600; 0.9364@410; 0.9827@530	*

(λ: Wavelength in nm; T: Temperature in centigrade, \*: Our work)

spectrophotometer analyzes the transmittance and the absorbance as the measurement of the transmittance and/or absorbance by adjusting a specific wavelength to the sample with a blank sample for calibration, these measurements use the beer's law Eq. (3). However, image processing is the basis of the application and the linear response in image processing comes with more computational complexity than with laboratory instruments used. Due to the promising results from plasmonic nanosensors, we dedicate future efforts to merge both hardware implementation with the reported software here to investigate further advancements in the smartphone sensing environment [36]. The colorimetric sensing application provides highly compatible concentration measurements of the materials in comparison with the laboratory spectrophotometer. The novelty of our study lies in the accurate prediction of multiple biochemical materials concentrations in various lightning effects, reducing the measurement time in an easy-to-use portable environment without the need for internet access, as the colorimetric sensing application does not require feedback from the data center for concentration measurement, also the novel approach of incorporating powerful software to tackle various issues that might arise in the traditional measurements like power consumption, heating, and calibration. The ability to convey multiple tasks, prediction of concentration, measurement of both absorbance and transmittance, with error estimation charts and R<sup>2</sup> values reporting within the colorimetric sensing application as far as our knowledge there has not been any application that can provide all the capabilities of our application. For comprehension (Table 1) shows a comparative analysis of the relevant literature with different approaches to the concentration calculation. As indicated in (Table 1) no study has reported both absorbance and transmittance with three different biochemical materials and a comparison with a spectrophotometer for reference, besides, our compatible and reliable prediction of the concentration is very compelling. We intend to progress our research by adapting the whole sensor system composed of the smartphone 3D printed adapter with lenses, filters, and both light-emitting diodes (LEDs) and Lasers as illumination sources.

## 6. Conclusions

The colorimetric sensing application developed here can be a good candidate for a variety of biochemical materials that enable the interested users to perform rapid testing and measurement of material concentration based on the simple image capturing of the carefully prepared samples. We believe that continuing this approach is of interest to rapid test, measurement, detection, and diagnosis studies that rely on the concept of colorimetry. The efficiency and reliability of the colorimetric sensing application with high accuracy concentration prediction is a promising application that can benefit researchers worldwide.

## Declaration of Competing Interest

The authors have declared no conflict of interest.

## Acknowledgments

We would like to acknowledge the laboratory technician Mr. Sadiq Hamoudi for assisting us with sample preparation and the anonymous reviewers for their efforts.

## Funding

This work was funded by the MAECI Grants: Study in Italy. Italian Ministry of Foreign Affairs and International Cooperation (Rome, Lazio), Grant Number: 1601461393.

## Appendix A. Supplementary data

Supplementary data to this article can be found online at <https://doi.org/10.1016/j.sbsr.2021.100404>.

## References

- [1] T. Alawsi, Z. Al-Bawi, A review of smartphone point-of-care adapter design, Eng. Reports 1 (2) (2019). Sep.
- [2] J.-Y. Yoon, Basic principles of optical biosensing using a smartphone, Smartphone Based Med. Diagn. (2020) 11–28.
- [3] Benjamin Jin Seong Ch'ng, Development of Smartphone-Based Spectroscopy Instruments for Diagnostic Test Analysis, 2015, p. 14778. Graduate Theses and Dissertations.
- [4] C.K. Kuşçuoğlu, H. Güner, M.A. Söylemez, O. Güven, M. Barsbay, A smartphone-based colorimetric PET sensor platform with molecular recognition via thermally initiated RAFT-mediated graft copolymerization, Sensors Actuators B Chem. 296 (2019) 126653. Oct.
- [5] V. Kılıç, N. Horzum, M. Ertugrul Solmaz, From sophisticated analysis to colorimetric determination: smartphone spectrometers and colorimetry. Color Detect., 2020. Apr.
- [6] H.-C. Wang, F.-Y. Chang, T.-M. Tsai, Design, fabrication, and feasibility analysis of a colorimetric detection system with a smartphone for self-monitoring blood glucose, J. Biomed. Opt. 24 (02) (2019) 1. Feb.
- [7] H.-C. Wang, F.-Y. Chang, T.-M. Tsai, C.-H. Chen, Y.-Y. Chen, Development and clinical trial of a smartphone-based colorimetric detection system for self-monitoring of blood glucose, Biomed. Optics Express 11 (4) (2020) 2166. Mar.
- [8] G. Xiao, J. He, X. Chen, Y. Qiao, F. Wang, Q. Xia, L. Yu, Z. Lu, A wearable, cotton thread/paper-based microfluidic device coupled with smartphone for sweat glucose sensing, Cellulose 26 (7) (2019) 4553–4562. Apr.
- [9] C.-S. Chuang, C.-Z. Deng, Y.-F. Fang, H.-R. Jiang, P.-W. Tseng, H.-J. Sheen, Y.-J. Fan, A smartphone-based diffusometric immunoassay for detecting c-reactive protein, Sci. Rep. 9 (1) (2019). Nov.
- [10] L. Zhong, J. Sun, Y. Gan, S. Zhou, Z. Wan, Q. Zou, K. Su, P. Wang, Portable smartphone-based colorimetric analyzer with enhanced gold nanoparticles for on-site tests of seafood safety, Anal. Sci. 35 (2) (2019) 133–140. Feb.

- [11] G.S. Luka, E. Nowak, J. Kawchuk, M. Hoorfar, H. Najjaran, Portable device for the detection of colorimetric assays, *R. Soc. Open Sci.* 4 (11) (2017) 171025. Nov.
- [12] N. Lopez-Ruiz, V.F. Curto, M.M. Erenas, F. Benito-Lopez, D. Diamond, A.J. Palma, L.F. Capitan-Vallvey, Smartphone-based simultaneous pH and nitrite colorimetric determination for paper microfluidic devices, *Anal. Chem.* 86 (19) (2014) 9554–9562. Sep.
- [13] A. Lace, D. Ryan, M. Bowkett, J. Cleary, Chromium monitoring in water by colorimetry using optimised 1,5-diphenylcarbazide method, *Int. J. Environ. Res. Public Health* 16 (10) (2019) 1803. May.
- [14] M.L. Firdaus, W. Alwi, F. Trinoveldi, I. Rahayu, L. Rahmidar, K. Warsito, Determination of chromium and iron using digital image-based colorimetry, *Procedia Environ. Sci.* 20 (2014) 298–304.
- [15] M.L. Firdaus, A. Aprian, N. Meileza, M. Hitsmi, R. Elvia, L. Rahmidar, R. Khaydarov, Smartphone coupled with a paper-based colorimetric device for sensitive and portable mercury ion sensing, *Chemosensors* 7 (2) (2019) 25. May.
- [16] X. Huang, D. Xu, J. Chen, J. Liu, Y. Li, J. Song, X. Ma, J. Guo, Smartphone-based analytical biosensors, *Analyst* 143 (22) (2018) 5339–5351.
- [17] M. Pohanka, Colorimetric hand-held sensors and biosensors with a small digital camera as signal recorder, a review, *Rev. Anal. Chem.* 39 (1) (2020) 20–30. Jul.
- [18] B. Coleman, C. Coarsey, W. Asghar, Cell phone based colorimetric analysis for point-of-care settings, *Analyst* 144 (6) (2019) 1935–1947.
- [19] M. Sarwar, J. Leichner, G.M. Naja, C.-Z. Li, Smart-phone, paper-based fluorescent sensor for ultra-low inorganic phosphate detection in environmental samples, *Microsyst Nanoeng.* 5 (1) (2019). Oct.
- [20] M.E. Quimbar, K.M. Kremek, A.R. Lippert, A chemiluminescent platform for smartphone monitoring of H<sub>2</sub>O<sub>2</sub> in human exhaled breath condensates, *Methods* 109 (2016) 123–130. Oct.
- [21] Y. Xing, Q. Zhu, X. Zhou, P. Qi, A dual-functional smartphone-based sensor for colorimetric and chemiluminescent detection: A case study for fluoride concentration mapping, *Sensors Actuators B Chem.* 319 (2020) 128254. Sep.
- [22] A.S. Paterson, B. Raja, V. Mandadi, B. Townsend, M. Lee, A. Buell, B. Vu, J. Brgoch, R.C. Willson, A low-cost smartphone-based platform for highly sensitive point-of-care testing with persistent luminescent phosphors, *Lab Chip* 17 (6) (2017) 1051–1059.
- [23] H. Sun, S. Liu, W. Lin, K.Y. Zhang, W. Lv, X. Huang, F. Huo, H. Yang, G. Jenkins, Q. Zhao, W. Huang, Smart responsive phosphorescent materials for data recording and security protection, *Nat. Commun.* 5 (1) (2014). Apr.
- [24] H. Kim, Y. Jung, I.-J. Doh, R.A. Lozano-Mahecha, B. Applegate, E. Bae, Smartphone-based low light detection for bioluminescence application, *Sci. Rep.* 7 (1) (2017). Jan.
- [25] J.I. Hong, B.-Y. Chang, Development of the smartphone-based colorimetry for multi-analyte sensing arrays, *Lab Chip* 14 (10) (2014) 1725–1732.
- [26] Y. Jung, J. Kim, O. Awofeso, H. Kim, F. Regnier, E. Bae, Smartphone-based colorimetric analysis for detection of saliva alcohol concentration, *Appl. Opt.* 54 (31) (2015) 9183. Oct.
- [27] A.Y. Mutlu, V. Küçük, G.K. Özdemir, A. Bayram, N. Horzum, M.E. Solmaz, Smartphone-based colorimetric detection via machine learning, *Analyst* 142 (13) (2017) 2434–2441.
- [28] X.-L. Guo, Y. Chen, H.-L. Jiang, X.-B. Qiu, D.-L. Yu, Smartphone-based microfluidic colorimetric sensor for gaseous formaldehyde determination with high sensitivity and selectivity, *Sensors* 18 (9) (2018) 3141. Sep.
- [29] A. Soni, R.K. Surana, S.K. Jha, Smartphone based optical biosensor for the detection of urea in saliva, *Sensors Actuators B Chem.* 269 (2018) 346–353. Sep.
- [30] U. Brackmann, Lambdachrome® laser dyes, in: *Lambda Physik AG-D-37079 Goettingen, Germany, 3rd ed.*, 2000.
- [31] A. Toor, A. Toor, K. Khalighi, M. Krishnamurthy, Triglyceride levels greater than 10,000 mg/dL in a 49-year-old female without evidence of pancreatitis, *Case Rep. Endocrinol.* 2019 (2019).
- [32] A. Tirosh, I. Shai, R. Bitzur, I. Kochba, D. Tekes-Manova, E. Israeli, T. Shochat, A. Rudich, Changes in triglyceride levels over time and risk of type 2 diabetes in young men, *Diabetes Care* 31 (10) (2008) 2032–2037.
- [33] U. Laufs, K.G. Parhofer, H.N. Ginsberg, R.A. Hegele, Clinical review on triglycerides, *Eur. Heart J.* 41 (1) (2020) 99–109.
- [34] D. Daniel, P. Hardigan, A. Jawaid, R. Bhandari, M. Daniel, The effect of elevated triglycerides on the onset and progression of coronary artery disease: a retrospective chart review, *Cholesterol* 2015 (2015).
- [35] Cleveland Clinic [online]. <https://my.clevelandclinic.org/health/articles/11117-triglycerides>. (Accessed 31 January 2020).
- [36] A.W. Jabar, Z.F. Al-Bawi, R.A. Faris, H.K. Wahhab, Plasmonic nanoparticles decorated salty paper based on sers platform for diagnostic low-level contamination: lab on paper, *Iraqi J. Laser* 18 (1) (2019) 43–49.
- [37] S. Ait Errayess, L. Idrissi, A. Amine, Smartphone-based colorimetric determination of sulfadiazine and sulfasalazine in pharmaceutical and veterinary formulations, *Instrum. Sci. Technol.* 46 (6) (2018) 656–675. Mar.
- [38] R. Bogucki, M. Greggila, P. Mallory, J. Feng, K. Siman, B. Khakpoor, H. King, A. W. Smith, A 3D-printable dual beam spectrophotometer with multiplatform smartphone adaptor, *J. Chem. Educ.* 96 (7) (2019) 1527–1531. Jun.
- [39] B.S. Hosker, Demonstrating principles of spectrophotometry by constructing a simple, low-cost, functional spectrophotometer utilizing the light sensor on a smartphone, *J. Chem. Educ.* 95 (1) (2017) 178–181. Nov.
- [40] T.S. Kuntzleman, E.C. Jacobson, Teaching beer's law and absorption spectrophotometry with a smart phone: a substantially simplified protocol, *J. Chem. Educ.* 93 (7) (2016) 1249–1252. Jan.
- [41] A. Shahvar, D. Shamsaei, M. Saraji, A portable smartphone-based colorimetric sensor for rapid determination of water content in ethanol, *Measurement* 150 (2020) 107068. Jan.
- [42] D.-H. Park, J.-M. Heo, W. Jeong, Y.H. Yoo, B.J. Park, J.-M. Kim, Smartphone-based VOC sensor using colorimetric polydiacetylenes, *ACS Appl. Mater. Interfaces* 10 (5) (2018) 5014–5021. Jan.



**Taif Alawsi:** He is a Ph.D. student at the University of Baghdad, Institute of Laser for Postgraduate Studies, Electronics and Communication Engineering. Currently, he is a Ph.D. Researcher at the Sapienza University of Rome, Department of Information Engineering, Electronics and Telecommunications, Rome, Italy. He is a certified reviewer for Web of Science and Scopus indexed journals with 41 records for 10 journals. He is a member of IEEE, IEEE Photonics Society, American Chemical Society, Optical Society of America, Italian Society of Optics and Photonics, and Iraqi Engineering Union. His research interests include Optics, Lasers, Photonics, Solar cells, Graphene, Smartphone Sensors, and Image Processing.



**Gabriele Proietti Mattia:** Obtained his bachelor's and master's degree in Computer Engineering in 2017 and 2019 respectively at the La Sapienza University of Rome. Now he is a Ph.D. student in Computer Engineering and his research interests concern the architectures and algorithms for Cloud and Fog infrastructures.



**Zainab Al-Bawi:** Received her B.Sc. in Physics from Al Mustansiriya University, in 1992, M.Sc. in Laser from the University of Technology, Iraq in 1997, and her Ph.D. in Physics from the University of Baghdad, in 2004. She was a joint researcher at the University of Sussex, UK and she was a visiting researcher at the University of Milan, Italy. She teaches Ph.D. and M.Sc. classes at the Institute of Laser for postgraduate studies including optics, spectroscopy, laser-material interaction, and applied optics. She supervised more than 15 Ph.D. and M.Sc. Thesis. Currently, she is an associate professor at the University of Baghdad, Institute of Laser for postgraduate studies. She had more than 41 published articles both local and international publications. Her research interests include sensors, biosensors, spectroscopy, nonlinear spectroscopy, electrochemical sensors, and nanotechnology.



**Roberto Beraldì:** He is a professor of computer science at the La Sapienza University of Rome, he has more than 140 published papers in peer-reviewed journals and conference proceedings. He supervised many Ph.D. and M.Sc. students. He teaches many courses including mobile application and cloud computing.